Special issue article

Journal of Physical Organic Chemistry

Received: 10 June 2016, Accepted: 26 June 2016, Published online in Wiley Online Library

(wileyonlinelibrary.com) DOI: 10.1002/poc.3621

Dinitreno pentaradicals: organic sextet molecules

Joel Mieres-Pérez[a], Stefan Henkel[a], Enrique Mendez-Vega[a], Tim Schleif[a], Thomas Lohmiller[b,a], Anton Savitsky[b] and Wolfram Sander[a]*

A new sextet ground state molecule, the 2,4,6-trichloro-1,3-dinitrenophenoxyl radical, was obtained upon UV photolysis of the corresponding diazido precursor in argon at 5 K. The sextet molecule is formed stepwise with the triplet nitrene, the quartet nitreno radical, and the quintet dinitrene as intermediates that were detected by EPR spectroscopy. IR and UV–Vis measurements only allowed us to observe the main product, the quintet dinitrene. The coupling between the two nitrene centers and the oxygen centered radical in the sextet state results in zero-field splitting (zfs) parameters of $|D/hc| = 0.088\ cm^{-1}$ and $|E/hc| = 0.009\ cm^{-1}$, considerably larger than in previously reported organic sextet molecules. An analogous sextet dinitrene formed by replacing the oxygen centered radical by a carbon centered radical was also studied by EPR spectroscopy, and in this case the zfs parameters $|D/hc| = 0.125\ cm^{-1}$ and $|E/hc| = 0.023\ cm^{-1}$ indicate even larger spin localization.

Keywords: EPR; matrix isolation; nitrenes; organic radicals; sextet

INTRODUCTION

The magnetic properties of organic polyradicals have attracted the attention of the scientific community for many years, as these species are discussed as building blocks for organic magnetic materials.[1–7] Among the organic high-spin molecules reported so far, only very few exhibit a sextet ($S = 5/2$) spin state.[8,9] Rajca et al.[8] synthesized pentaradical **P1** with benzyl radical units as spin bearing centers (Chart 1). Using SQUID magnetometry they found $S \geq 2.3$. In the EPR spectra, two sets of signals corresponding to $S = 5/2$ and zero field splitting (zfs) parameters of $|D/hc| = 0.0027\ cm^{-1}$, $|E/hc| = 0.0009\ cm^{-1}$ and $|D/hc| = 0.0027\ cm^{-1}$, $|E/hc| = 0.0000\ cm^{-1}$, respectively, were assigned to two conformers of the pentaradical **P1**. Two years later, Fujita et al.[9] reported on the stable pentaradical **P2**, based on nitroxyl radicals. **P2** shows a sextet ground state with zfs parameters of $|D/hc| = 0.0039\ cm^{-1}$ and $|E/hc| = 0.0013\ cm^{-1}$. The structure of **P2** was determined by X−ray structure analysis.

Among organic polyradicals, nitrenes exhibit the largest D values and the strongest ferromagnetic exchange interactions between the unpaired electrons. In addition, nitrenes have large energy gaps (5–10 kcal/mol) between the high-spin ground state and low-spin excited states.[10] Therefore, they are well suited as molecular models for organic molecular magnets.[11] The design of a pentaradical based on nitrenes, rather than on carbon-centered radicals, is of high interest since such pentaradicals are expected to show considerably larger D values than the carbon-centered pentaradicals.

In order to synthesize a sextet pentaradical bearing two nitrene units and a single radical center, a 1,3-dinitrene phenyl motive with ferromagnetic coupling between the nitrene units was chosen as basis. As additional radical center, a phenoxyl radical as in 2,4,6-trichloro-1,3-dinitreno-phenoxyl radical **1** or a benzyl radical as in **2** were selected (Chart 2). The chlorine substituents in **1** are expected to efficiently suppress rearrangements of the phenylnitrene units to seven-membered ring systems according to Scheme 1.

EXPERIMENTAL SECTION

Matrix isolation spectroscopy

Matrix isolation experiments were performed by standard techniques as reported previously.[12,13] The matrices were generated by co-deposition of the precursors and a large excess of argon (Messer Griesheim, 99.99%).

Pulse EPR spectroscopy in frozen solution

Sample preparation

Compound **3** was dissolved in methylcyclohexane, and oxygen was removed by purging the solution with argon. 3 μl of the solution were transferred into a 0.4 mm inner diameter quartz tube for W-band measurements, and 30 μl were transferred into a Q-band quartz capillary EPR tube with an inner diameter of 1.6 mm. For UV irradiation a high pressure mercury lamp with quartz optics (L.O.T. Oriel) was used.

---

* *Correspondence to: Wolfram Sander, Lehrstuhl für Organische Chemie II, Ruhr-Universität Bochum, D-44780 Bochum, Germany.*
E-mail: wolfram.sander@rub.de

a *J. Mieres-Pérez, S. Henkel, E. Mendez-Vega, T. Schleif, T. Lohmiller, W. Sander*
Lehrstuhl für Organische Chemie II, Ruhr-Universität Bochum, D-44780, Bochum, Germany

b *T. Lohmiller, A. Savitsky*
Max-Planck-Institut für Chemische Energiekonversion, D-45470, Mülheim an der Ruhr, Germany

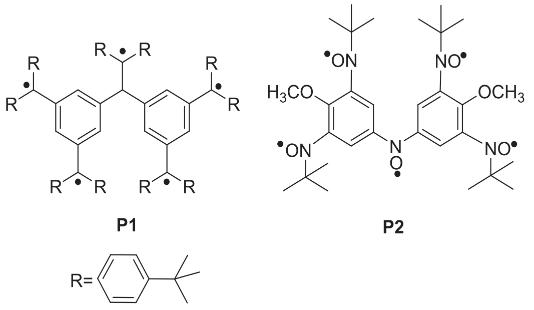

Chart 1. Previously reported organic sextet ground state molecules

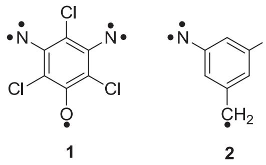

Chart 2. Pentaradicals studied in this work

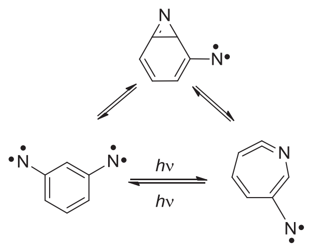

Scheme 1. Ring expansion process in nitrenes

Q-band and W-band pulse EPR spectroscopy

Q-band (≈34 GHz) pulse EPR experiments were performed at 5 K using a Bruker ELEXSYS E580 spectrometer equipped with a homebuilt TE$_{011}$ microwave cavity[14] and a cryogen-free closed-cycle cryostat (Cryogenic Limited) with a Cryomech liquid He compressor. W-band (≈94 GHz) pulse EPR measurements were carried out at 5 K using a Bruker ELEXSYS E680 spectrometer employing a homebuilt microwave cavity, which comprised a solenoid of Teflon-coated silver wire integrated into a commercial W-band probe head (Bruker). ESE-detected field-swept EPR spectra were recorded by use of the pulse sequence $\pi/2$-τ-π-τ-echo[15] with microwave pulse lengths $\pi = 40$ ns and inter-pulse distances $\tau = 300$ ns (Q-band) and 200 ns (W-band).

MATERIALS

1,3-Diazido-2,4,6-trichloro-5-fluorobenzene

1,3-Diazido-2,4,6-trichloro-5-fluorobenzene was prepared by a modified literature procedure[16] (see SI).

^{13}C-NMR (50 MHz, CDCl$_3$): $\delta = 153.8$ ppm (C5, d, $J = 250.7$ Hz), 134.7 (C1/C3, d, $J = 1.9$ Hz), 119.6 (C2, d, $J = 4.2$ Hz), 114.9 (C4/C6, d, $J = 21.1$ Hz). MS (EI, 70 eV): m/z (rel. int.) = 284 (8), 282 (25) [M]$^+$, 280 (27), 256 (9), 254 (41) [M − N$_2$]$^+$, 252 (42), 224 (3) [M − 2 N$_2$]$^+$, 191 (65), 189 (100) [M − 2 N$_2$ − Cl]$^+$, 165 (30), 163 (50), 154 (18) [M − 2 N$_2$ − 2Cl]$^+$, 128 (36), 47 (32), 31 (27). HRMS (EI-TOF) calculated for $C_6Cl_3FN_6$ 279.93492; Found: 279.92341. IR (Nujol): $\tilde{\nu}$ = 2220 m cm^{-1}, 2168 s, 2121vs (N$_3$), 1572 m, 1555 m, 1537 m (C = C), 1415vs (C–F), 1256 m, 1237 m, 1207 m, 958w, 808 m, 789 m, 525w.

1-(Allyloxy)-3,5-diazido-2,4,6-trichlorobenzene (3)

0.163 g (1.45 mmol) of KOtBu were suspended in 2 ml of dry dioxane. 0.13 ml (0.111 g, 1.90 mmol) of 2-propenol were added and the suspension was stirred for 15 min at room temperature upon which the mixture turned intense yellow. 0.140 g (0.50 mmol) of 1,3-diazido-2,4,6-trichloro-5-fluorobenzene were added and the reaction mixture was stirred for 3.5 h at room temperature. 5 ml of destilled water were added to the orange solution and it was stirred for 10 min at room temperature before extraction with MTBE. Evaporation of the solvent gave 0.135 g of orange-brown oil as crude product, which was purified by HPLC with hexane as eluent to give 0.045 g (0.14 mmol, 28% yield) of **3** as colorless solid.

^{1}H-NMR (200 MHz, CDCl$_3$): $\delta = 6.12$ ppm (ddt, $J = 16.3$, 10.3, 6.0 Hz, 1H, CH = CH$_2$), 5.43 (dd, $J = 17.1$, 1.4 Hz, 1H, CH = CH$_{trans}$), 5.32 (dd, $J = 10.3$, 1.2 Hz, 1H, CH = CH$_{cis}$), 4.54 (dt, $J = 6.0$, 1.2 Hz, 2H, OCH$_2$). ^{13}C-NMR (50 MHz, CDCl$_3$): $\delta = 151.5$ ppm (C1), 134.5 (C3/C5), 132.3 (CH = CH$_2$), 122.3 (C2/C6), 120.0 (C4), 119.8 (CH = CH$_2$), 74.9 (OCH$_2$). MS (EI, 70 eV): m/z (rel. int.) = 322 (1), 320 (3), 318 (3) [M]$^+$, 294 (1), 292 (3), 290 (3) [M − N$_2$]$^+$, 225 (2), 223 (5), 221 (4) [M − 2 N$_2$ − C$_3$H$_5$]$^+$, 197 (2), 195 (4), 193 (4) [M − 2 N$_2$ − C$_3$H$_5$ − CO]$^+$, 134 (6), 132 (8), 120 (7), 85 (5), 73 (6), 41 (100) [C$_3$H$_5$]$^+$, 39 (25) [C$_3$H$_3$]$^+$, 28 (7) [N$_2$/CO]$^+$. HRMS (EI-TOF) calculated for $C_9H_5Cl_3N_6O$ 317.91274; Found: 317.95904.

3,5-Diaminobenzyl alcohol

3,5-Diaminobenzyl alcohol was prepared according to a modified literature procedure[17] (see SI).

^{1}H-NMR (200 MHz, DMSO-d$_6$): $\delta = 5.77$ ppm (d, $J = 1.7$ Hz, 2H, H2/H6), 5.68 (t, $J = 1.8$ Hz, 1H, H4), 4.79 (t, $J = 5.8$ Hz, 1H, OH), 4.61 (s, 4H, NH$_2$), 4.19 (d, $J = 5.7$ Hz, 2H, CH$_2$OH).

3,5-Diazidobenzyl alcohol

3,5-Diazidobenzyl alcohol was prepared by a modified literature procedure[17] (see SI).

^{1}H-NMR (250 MHz, CDCl$_3$): $\delta = 6.83$ ppm (d, $J = 1.9$ Hz, 2H, H2/H6), 6.57 (t, $J = 1.9$ Hz, 1H, H4), 4.69 (d, $J = 3.5$ Hz, 2H, CH$_2$OH). ^{13}C-NMR (62.5 MHz, CDCl$_3$): $\delta = 144.7$ ppm (C3/C5), 142.2 (C1), 113.6 (C2/C6), 109.1 (C4), 64.5 (CH$_2$OH). MS (EI, 70 eV): m/z (rel. int.) = 190 (30)[M]$^+$, 162 (24) [M − N$_2$]$^+$, 155 (20), 133 (6) [M − 2 N$_2$ − H]$^+$, 121 (24), 107 (35) [M − 2 N$_3$ + H]$^+$, 105 (42) [M − 2 N$_3$ − H]$^+$, 79 (48), 64 (38), 52 (100) [C$_4$H$_4$]$^+$, 39 (55) [C$_3$H$_3$]$^+$, 31 (70) [CH$_2$OH]$^+$. HRMS (EI-TOF) calculated for $C_7H_6N_6O$ 190.01668; Found: 190.06031.

3,5-Diazidobenzyl mesylate

3,5-Diazidobenzyl mesylate was prepared following a literature procedure[18] (see SI).

^{1}H-NMR (400 MHz, CDCl$_3$): $\delta = 6.84$ ppm (d, $J = 1.8$ Hz, 2H, H2/H6), 6.67 (t, $J = 1.8$ Hz, 1H, H4), 5.17 (s, 2H, CH$_2$O), 3.02 (s, 3H, CH$_3$). ^{13}C-NMR (100 MHz, CDCl$_3$): $\delta = 142.6$ ppm (C3/C5), 137.2 (C1), 115.3 (C2/C6), 110.4 (C4), 69.7 (CH$_2$O), 38.4 (CH$_3$). MS (EI, 70 eV): m/z (rel. int.) = 268 (10) $[M]^+$, 240 (6) $[M - N_2]^+$, 185 (9), 173 (30) $[M - OMs]^+$, 133 (19), 116 (30), 105 (35), 79 (100) $[Ms]^+$, 63 (35), 52 (36) $[C_4H_4]^+$, 39 (30) $[C_3H_3]^+$. HRMS calculated for $C_8H_8N_6O_3S$ 267.96057; Found: 268.03786.

3,5-Diazidobenzyl iodide (**8**)

3,5-Diazidobenzyl iodide (**8**) was prepared according to a modified literature procedure[18] (see SI).

^{1}H-NMR (200 MHz, $CDCl_3$): $\delta = 6.80$ ppm (d, $J = 2.0$ Hz, 2H, H2/H6), 6.53 (t, $J = 2.0$ Hz, 1H, H4), 4.36 (s, 2H, CH_2I). ^{13}C-NMR (50 MHz, $CDCl_3$): $\delta = 142.9$ ppm (C3/C5), 142.2 (C1), 115.7 (C2/C6), 109.4 (C4), 3.0 (CH_2). MS (EI, 70 eV): m/z (rel. int.) = 300 (60) $[M]^+$, 272 (12) $[M - N_2]^+$, 173 (37) $[M - I]^+$, 127 (42) $[I]^+$, 117 (87) $[M - 2N_2 - I]^+$, 90 (92) $[C_7H_6]^+$, 63 (86), 52 (53), 39 (45). HRMS calculated for $C_7H_5N_6I$: 299.91390; Found: 299.96204.

Computational details

Geometry optimizations, vibrations analysis, and excited state calculations were carried out using the B3LYP and M06 functionals and the def2-TZVP basis set as implemented in Gaussian 09.[19] A spin-unrestricted formalism was used for the open-shell species. Tight convergence criteria for gradients and an integration grid having 99 radial shells per atom and 590 angular points per shell were used. Experimental EPR spectra were analyzed using the Easyspin program package.[20]

Calculations of the magnetic properties were conducted using the ORCA program package.[21] See SI for more detailed information.

RESULTS AND DISCUSSION

IR spectroscopy

1-(Allyloxy)-3,5-diazido-2,4,6-trichlorobenzene (**3**) was isolated in argon at 8 K, and its photochemistry was investigated by IR spectroscopy. The IR spectrum of matrix-isolated **3** shows the characteristic azide stretching vibration at 2124 cm^{-1}, which upon UV photolysis ($\lambda = 365$ nm) decreases in intensity. Simultaneously, new bands with the strongest absorptions at 1361, 1288, 940, and 786 cm^{-1} are formed. After prolonged photolysis (12 h) all IR absorptions of **3** disappear completely (Fig. 1). By comparison with DFT calculations, the new bands are assigned to the quintet dinitrene 2,4,6-trichloro-3,5-dinitreno-(allyloxy)-benzene **4**. The formation of larger amounts of rearranged products such as benzazirines or azepines can be excluded because the characteristic absorptions of these species in the region between 1650 and 1900 cm^{-1} are missing in the IR spectra. The characteristic azide stretching vibrations are bleached upon photolysis, which excludes the presence of triplet mononitrene **5**. Additional UV photolysis ($\lambda = 365$ nm) does not result in further changes in the spectrum, indicating that **4** is stable towards 365 nm irradiation. In particular, the allyl radical (Scheme 2) with its characteristic IR absorption at 801 cm^{-1}[22,23] is not formed under these conditions.

Further irradiation of the matrix with 266 nm light leads to a slight decrease of all remaining IR bands of **4** and appearance of a very low intensity band at 801 cm^{-1}. However, due to the low yield of O-allyl cleavage, other photoproducts, in particular **1**, could not be identified by IR spectroscopy.

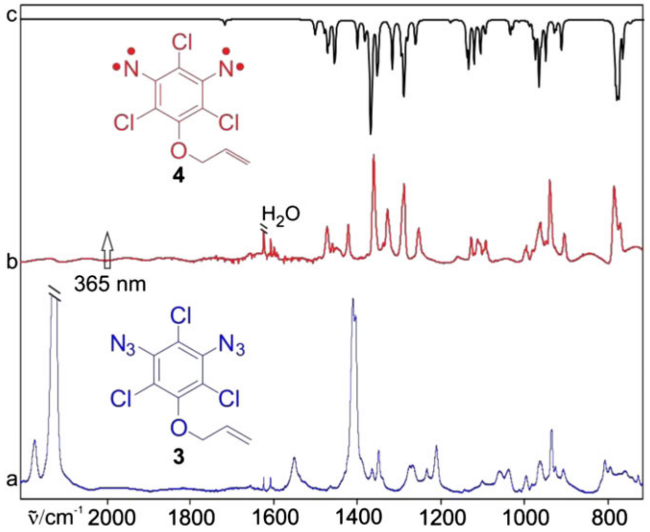

Figure 1. IR spectra showing the photochemistry of **3** in argon at 8 K. a) IR spectrum of **3**. b) IR spectrum obtained after 12 h irradiation of **3** with $\lambda = 365$ nm. c) Calculated IR spectrum of **4** (B3LYP/def2-TZVP). Three conformers of **4** with different orientations of the allyloxy group are considered (see SI for details)

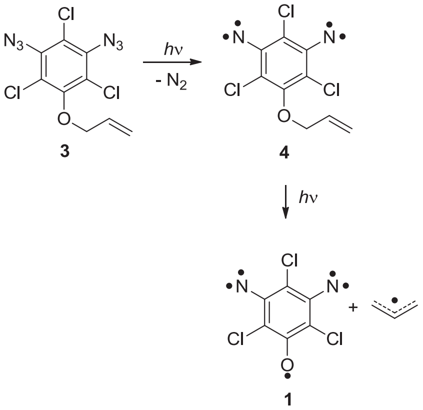

Scheme 2. Photochemistry of **3**

UV–Vis spectroscopy

Matrix-isolated **3** exhibits a broad band in the UV–Vis spectrum centered at 229 nm, which is decreasing in intensity on $\lambda = 365$ nm irradiation. Simultaneously, new bands with maxima at 481, 450, 327, 312, 285, 235, and 212 nm are formed. In order to analyze the UV–Vis data, TD-DFT calculations were carried out using a variety of functionals and basis sets. The best match with the experimental results was found for the quintet state of **4** calculated at the M06-2X/def2-TZVP level of theory. The calculation predicts the major electronic transitions of **4** at 404, 267, 226, and 207 nm, in reasonable agreement with the most intense observed bands (Fig. 2). However, the presence of other photoproducts as minor constituents of the matrix cannot be ruled out.

EPR spectroscopy

UV irradiation ($\lambda = 365$ nm) of **3** in argon at 5 K produces an EPR spectrum typical of quintet dinitrenes, which therefore is assigned to **4** (Fig. 3a). The signals at 66, 142, 308, 374, 460,

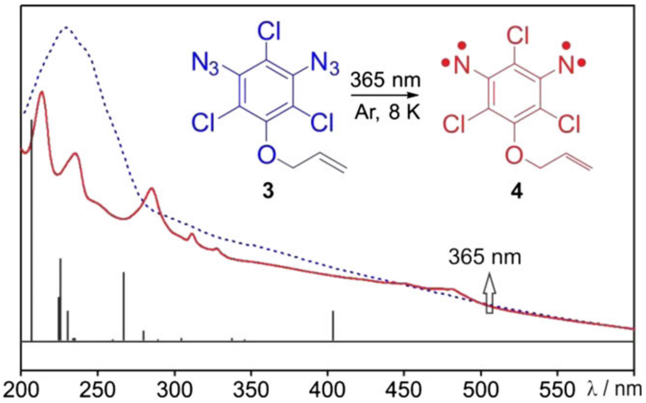

Figure 2. UV–Vis spectra showing the photochemistry of **3** in argon at 8 K. Dashed blue line: UV–Vis spectrum of **3**. Red solid line: UV–Vis spectrum obtained after 12 h of irradiation of **3** with $\lambda = 365$ nm. Black line: UV–Vis spectrum of **4**, calculated at the M06-2X/def2-TZVP level of theory

544, 613, 658, 848, and 946 mT are nicely reproduced by a simulation of a quintet species with zfs parameters of $|D/hc| = 0.190\ \text{cm}^{-1}$ and $|E/hc| = 0.043\ \text{cm}^{-1}$ (Fig. 3b). An additional line at 690 mT indicates the presence of triplet mononitrene **5** with $|D/hc| = 1.00\ \text{cm}^{-1}$ and $|E/hc| = 0.002\ \text{cm}^{-1}$. In agreement with the IR experiments, $\lambda = 365$ nm irradiation does not lead to products expected from the O-allyl cleavage. In particular, the absence of a strong signal around 342 mT indicates that the allyl radical is not formed.

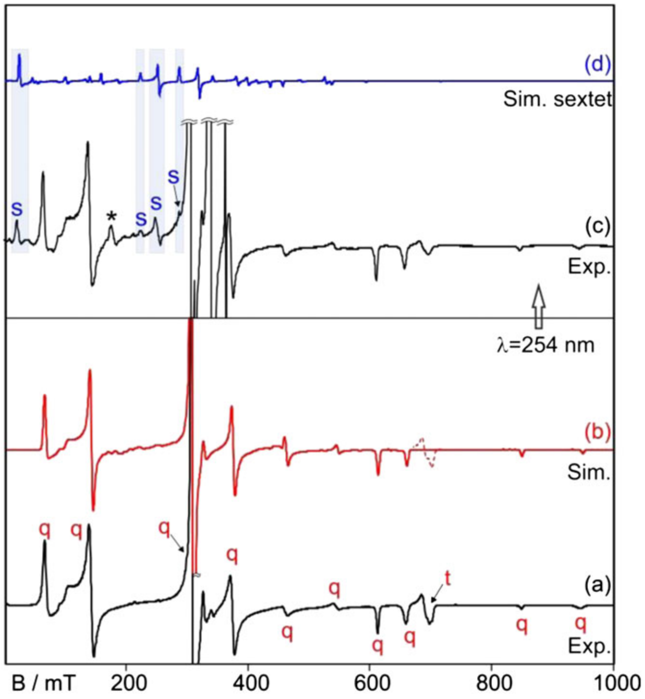

Figure 3. X-band CW EPR spectra of the photoproducts of matrix-isolated **3**. a) Spectrum obtained upon $\lambda = 365$ nm photolysis (50 min) of **3** in argon at 5 K. Lines assigned to the quintet are labeled as 'q', the triplet signal is labeled as 't'. b) Simulated spectrum of a quintet species with $|D/hc| = 0.190\ \text{cm}^{-1}$ and $|E/hc| = 0.043\ \text{cm}^{-1}$ ($\nu = 9.575$ GHz). A signal centered at 690 mT indicates the presence of a triplet nitrene with $|D/hc| = 1.00\ \text{cm}^{-1}$ and $|E/hc| = 0.002\ \text{cm}^{-1}$ (simulation shown as dashed line). c) Spectrum obtained after additional photolysis of the matrix with $\lambda = 254$ nm (1.5 h). Signals assigned to sextet species are labeled as 's'. The asterisk denotes an additional band that is attributed to a quartet species (see text for details). d) Simulated spectrum of a sextet species with $|D/hc| = 0.088\ \text{cm}^{-1}$ and $|E/hc| = 0.009\ \text{cm}^{-1}$ ($\nu = 9.678$ GHz)

Further photolysis of the matrix with $\lambda = 254$ nm leads to a decrease in intensity of all signals assigned to triplet **5** and quintet **4** and formation of signals at 22, 225, 255, and 290 mT. In addition, a strong radical signal centered at 342 mT and the characteristic transitions of hydrogen atoms at 315 and 365 mT are found (Fig. 3c). The new signals are assigned to sextet dinitreno phenoxyl radical **1** with the zfs parameters $|D/hc| = 0.088\ \text{cm}^{-1}$ and $|E/hc| = 0.009\ \text{cm}^{-1}$ obtained from a simulation (Fig. 3d). Because of overlap with the signals of quintet **4**, identification of further bands of **1** was not possible.

An additional signal at 177 mT indicates the formation of a quartet species. The quartet is assigned to **6** (Scheme 3), probably formed from precursor **3** by cleavage of only one azide group in addition to the O-allyl bond. The large concentration of quintet **4** in the matrix indicates that the major pathway is the cleavage of both azide groups. However, we cannot exclude that the quartet is a secondary photoproduct of sextet 1. Again, the over-

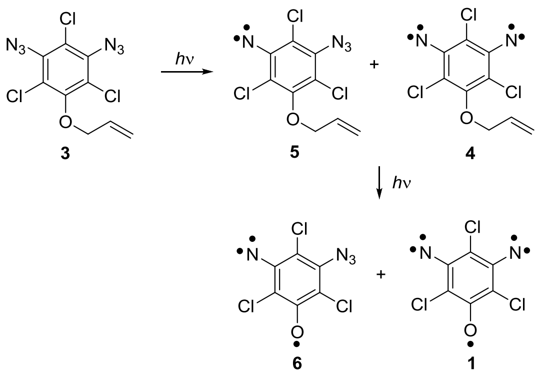

Scheme 3. Triplet, quartet, quintet, and sextet species formed by photolysis of **3**

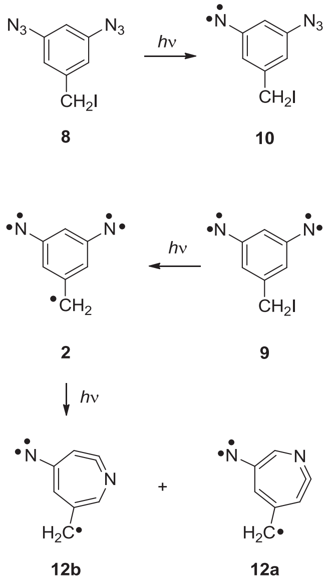

Scheme 4. Photochemistry of **8**

lap with the intense quintet signals precludes assignment of other signals of the quartet compound. The position of the transition assigned to the quartet species is not very sensitive to the D values, and therefore the zfs values cannot be determined reliably.

The photochemistry of precursor **3** in methylcyclohexane at 5 K was studied by W-band pulse EPR (Scheme 4). After UV photolysis, intense signals assigned to triplet mononitrene **5** were observed together with additional bands assigned to quintet **4**. The signals of **4** increased during overnight irradiation, while that of **5** decreased, but no signals could be assigned to **1** (Figure S1, SI). Simulations confirmed the zfs parameters from the X-band experiments, and especially the W-band simulations identified the sign of the D value of quintet **4** to be positive, $D/hc = 0.190\,\text{cm}^{-1}$ (Figure S2, SI).

In addition to **1**, the pentaradical **2**, in which the oxygen-centered radical is replaced by a carbon-centered radical, was investigated by X-band CW EPR spectroscopy. Photolysis of matrix-isolated **8** with $\lambda = 308$ nm leads to formation of a quintet species with transitions at 86, 146, 279, 309, 394, 623, and 860 mT (Fig. 4a). The spectrum could be simulated using the zfs parameters $|D/hc| = 0.205\,\text{cm}^{-1}$ and $|E/hc| = 0.041\,\text{cm}^{-1}$ (Fig. 4b) and was assigned to quintet **9** (Scheme 4). In addition to the quintet signals, a strong line centered at 340 mT indicates the formation of radical species by cleavage of the C-I bond of **8**. An intense line at 701 mT was assigned to triplet mononitrene **10** with a D value of approximately $1.00\,\text{cm}^{-1}$. Additional bands at 79, 178, 251, 268, and 568 mT are assigned to species containing a nitrene unit as well as a radical center as in **11** or **12** (Scheme 4). However, short-wavelength UV photolysis ($\lambda = 254$) nm leads to lines at 5, 202, 229 238, and 430 mT that are in agreement with a sextet species with zfs parameters of $|D/hc| = 0.125\,\text{cm}^{-1}$ and $|E/hc| = 0.023\,\text{cm}^{-1}$ (Fig. 4c,4d). Therefore, these signals are tentatively assigned to **2**.

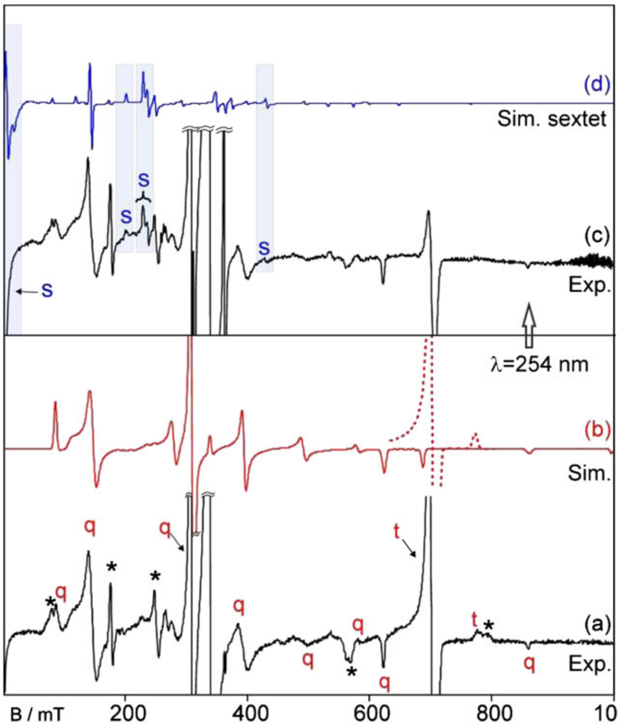

Figure 4. EPR spectra of the photoproducts of matrix-isolated **8**. a) Spectrum obtained upon $\lambda = 308$ nm photolysis (17 min) of **8** in argon at 5 K. Lines assigned to the quintet are labeled as 'q', triplet lines are labeled as 't'. b) Simulated spectrum of a quintet species with $|D/hc| = 0.205\,\text{cm}^{-1}$ and $|E/hc| = 0.041\,\text{cm}^{-1}$ ($\nu = 9.566$ GHz). A strong line centered at 701 mT indicates the presence of a triplet nitrene with $|D/hc| = 1.04\,\text{cm}^{-1}$ (simulation shown as dashed line). Asterisks denote additional bands that are attributed to quartet species (see text for details). c) Spectrum obtained after additional photolysis of the matrix with $\lambda = 254$ nm (1 h). Signals assigned to the sextet species are labeled as 's'. d) Simulated spectrum of a sextet species with $|D/hc| = 0.125\,\text{cm}^{-1}$ and $|E/hc| = 0.023\,\text{cm}^{-1}$ ($\nu = 9.564$ GHz)

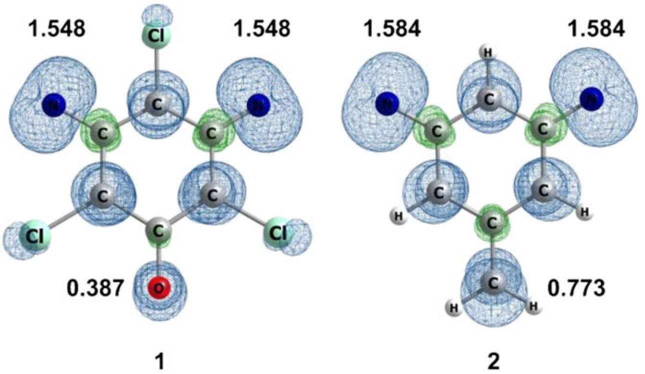

Figure 5. Spin density distribution of sextet pentaradicals **1** and **2**. Blue color indicates an excess of α-spin density at the atom (positive spin density), and green color shows an excess of β-spin density at the atom (negative spin density)

The calculated zfs parameters (see SI table TI) for sextets **1** ($|D/hc| = 0.093$) and **2** ($|D/hc| = 0.096$) follow the same trend as the ones obtained experimentally, that is, higher D values in the case of sextet **2** than for sextet **1**, which indicates a stronger localization of the electron density at the radical centers in the case of **2**. This is in agreement with the higher values of the calculated spin densities for **2** (Fig. 5).

CONCLUSION

Pentaradicals with sextet electronic ground states are interesting high spin species. Nitrenoradical **1** could be produced by photolysis of precursor **3** and characterized by EPR spectroscopy. Because the cleavage of the O-allyl group is very inefficient, only low yields of **1** were obtained, and therefore it was not possible to identify this pentaradical by the less sensitive UV–Vis or IR spectroscopy. Dinitrene **4**, on the other hand, was formed in very high yield and could therefore be observed by EPR, UV–Vis, and IR spectroscopy. The chlorine substituents inhibit the phototchemical rearrangement of the phenylnitrene derivatives **1**, **4**, **5**, or **6** to the corresponding keteneimines, and therefore high yields of nitrenes are achieved.

In contrast, nitrenes such as **9** or **10** can easily undergo photochemical rearrangements to keteneimines, and therefore the yields are low. Pentaradical **2** was therefore only investigated by EPR spectroscopy.

These sextet radicals **1** and **2** exhibit D values more than 10 times larger than previously reported organic sextets, indicating a large degree of spin-localization at the nitrene units. These sextet species could be used as new building blocks for the synthesis of organic magnetic materials.

Acknowledgements

This work was supported by the Cluster of Excellence RESOLV (EXC 1069) funded by the Deutsche Forschungsgemeinschaft (DFG).

REFERENCES

[1] I. Fujita, Y. Teki, T. Takui, T. Kinoshita, K. Itoh, F. Miko, Y. Sawaki, H. Iwamura, A. Izuoka, T. Sugawara, *J. Am. Chem. Soc.* **1990**, *112*, 4074.
[2] T. Ishida, H. Iwamura, *J. Am. Chem. Soc.* **1991**, *113*, 4238.
[3] K. Itoh, T. Takui, *Proc. Jpn. Acad. Ser. B.* **2004**, *80*, 29.
[4] B. B. Wright, M. S. Platz, *J. Am. Chem. Soc.* **1983**, *105*, 628.
[5] W. Adam, M. Baumgarten, W. Maas, *J. Am. Chem. Soc.* **2000**, *122*, 6735.
[6] S. J. Jacobs, D. A. Dougherty, *Angew. Chem. Int. Ed.* **1994**, *33*, 1104.
[7] L. B. Anatolii, *Russ. Chem. Rev.* **1990**, *59*, 307.
[8] A. Rajca, S. Rajca, S. R. Desai, *J. Am. Chem. Soc.* **1995**, *117*, 806.
[9] Y. M. J. Fujita, K. M. T. Matsuo, T. Akita, N. Koga, H. Iwamura, *Chem. Commun.* **1997**, 2393.
[10] E. Y. Misochko, D. V. Korchagin, K. V. Bozhenko, S. V. Chapyshev, S. M. Aldoshin, *J. Chem. Phys.* **2010**, *133*, 064101.
[11] S. V. Chapyshev, *Russ. Chem. Bull. Int. Ed.* **2012**, *60*, 1274.
[12] J. Mieres-Pérez, E. Mendez-Vega, K. Velappan, W. Sander, *J. Org. Chem.* **2015**, *80*, 11926.
[13] P. Costa, W. Sander, *Angew. Chem. Int. Ed.* **2014**, *53*, 5122.
[14] E. Reijerse, F. Lendzian, R. Isaacson, W. Lubitz, *J. Magn. Reson.* **2012**, *214*, 237.
[15] E. L. Hahn, *Phys. Rev.* **1950**, *80*, 580.
[16] S. V. Chapyshev, A. V. Chernyak, *J. Fluorine Chem.* **2013**, *156*, 303.
[17] N. Umezawa, N. Matsumoto, S. Iwama, N. Kato, T. Higuchi, *Bioorg. Med. Chem.* **2010**, *18*, 6340.
[18] T. Hosoya, A. Inoue, T. Hiramatsu, H. Aoyama, T. Ikemoto, M. Suzuki, *Bioorg. Med. Chem.* **2009**, *17*, 2490.
[19] G. W. T. M. J. Frisch, H. B. Schlegel, G. E. Scuseria, M. A. Robb, J. R. Cheeseman, G. Scalmani, V. Barone, B. Mennucci, G. A. Petersson, H. Nakatsuji, M. Caricato, X. Li, H. P. Hratchian, A. F. Izmaylov, J. Bloino, G. Zheng, J. L. Sonnenberg, M. Hada, M. Ehara, K. Toyota, R. Fukuda, J. Hasegawa, M. Ishida, T. Nakajima, Y. Honda, O. Kitao, H. Nakai, T. Vreven, J. A. Montgomery Jr. , J. E. Peralta, F. Ogliaro, M. Bearpark, J. J. Heyd, E. Brothers, K. N. Kudin, V. N. Staroverov, R. Kobayashi, J. Normand, K. Raghavachari, A. Rendell, J. C. Burant, S. S. Iyengar, J. Tomasi, M. Cossi, N. Rega, J. M. Millam, M. Klene, J. E. Knox, J. B. Cross, V. Bakken, C. Adamo, J. Jaramillo, R. Gomperts, R. E. Stratmann, O. Yazyev, A. J. Austin, R. Cammi, C. Pomelli, J. W. Ochterski, R. L. Martin, K. Morokuma, V. G. Zakrzewski, G. A. Voth, P. Salvador, J. J. Dannenberg, S. Dapprich, A. D. Daniels, Ö. Farkas, J. B. Foresman, J. V. Ortiz, J. Cioslowski, D. J. Fox, Gaussian, Inc., Wallingford CT, **2009**, Revision D.01 ed., Gaussian, Inc., Wallingford CT, **2009**.
[20] S. Stoll, A. Schweiger, *J. Magn. Reson.* **2006**, *178*, 42.
[21] F. Neese, *Wiley Interdiscip. Rev. Comput. Mol. Sci.* **2012**, *2*, 73.
[22] M. E. Jacox, D. E. Milligan, *Chem. Phys.* **1974**, *4*, 45.
[23] S. Nandi, P. A. Arnold, B. K. Carpenter, M. R. Nimlos, D. C. Dayton, G. B. Ellison, *J. Phys. Chem. A.* **2001**, *105*, 7514.

SUPPORTING INFORMATION

Additional supporting information can be found in the online version of this article at the publisher's website.